Fusarium verticillioides FvPex8 is a key component of peroxisomal docking/translocation module that serves important roles in fumonisin biosynthesis but not in virulence

Wenying Yu[1,2], Mei Lin[1], Minghui Peng[2], Huijuan Yan[3], Jie Zhou[1,2], Guodong Lu[2], Won Bo Shim[3*] and Zonghua Wang[2*]

1 Key Laboratory of Biopesticide and Chemical Biology of Ministry of Education & Fujian Universities Key Laboratory for Plant-Microbe Interaction, College of Life Science,Fujian Agriculture and Forestry University, Fuzhou 350002, China

2 State Key Laboratory of Ecological Pest Control for Fujian and Taiwan Crops, College of Plant Protection, Fujian Agriculture and Forestry University, Fuzhou 350002, China

3 Department of Plant Pathology and Microbiology, Texas A&M University, College Station, TX 77843-2132, USA

Co-corresponding authors

Won Bo Shim; TEL: +1 979 458 2190, Email: wbshim@tamu.edu

Zonghua Wang; Tel: +86 591 83789202, Email: wangzh@fafu.edu.cn

Abstract

Peroxisomes are ubiquitous organelles in eukaryotic cells that fulfill various important metabolic functions. In this study, we investigated the role of Docking/Translocation Module (DTM) peroxins, mainly FvPex8, FvPex13, FvPex14, and FvPex33, in *Fusarium verticillioides* virulence and fumonisin B1 (FB1) biosynthesis. Protein interaction experiments suggested that FvPex13 serves as the core subunit of *F. verticillioides* DTM. When we generated gene deletion mutants (ΔFvpex8, ΔFvpex13, ΔFvpex14, ΔFvpex33, ΔFvpex33/14) and examined whether the expression of other peroxin genes were affected in the DTM mutants, ΔFvpex8 strain showed most drastic changes to *PEX* gene expression profiles. Deletion mutants exhibited disparity in carbon source utilization and defect in cell wall integrity when stress agents were applied. Under nutrient starvation, mutants also showed higher levels of lipid droplet accumulation. Notably, ΔFvpex8 mutant showed significant FB1 reduction and altered expression of *FUM1* and *FUM19* genes. However, FvPex13 was primarily responsible for virulence, while ΔFvpex33/14 double mutant also showed virulence defect. In summary, our study suggests that FvPex13 is the core component of DTM, regulating peroxisome membrane biogenesis as well as PTS1- and PTS2-mediated transmembrane cargo transportation. Importantly, we predict FvPex8 as a key component in DTM that affects peroxisome function in FB1 biosynthesis in *F. verticillioides*.

Key words: *F. verticillioides,* docking/translocation module, peroxins, fumonisin B1, virulence

Introduction

Peroxisomes are a family of membrane-bound microbodies found in all major eukaryotes, with specific metabolic properties showing substantial differences among various species and tissue types (Alberts *et al.*, 2002, Cooper, 2000). These cellular organelles, including peroxisomes, glyoxysomes in plants and fungi, glycosomes in trypanosomes, and Woronin bodies in filamentous fungi, are involved in a variety of important cellular functions, including fatty acid metabolism, reactive oxygen species detoxification, and secondary metabolite biosynthesis (Saikia & Scott, 2009, Imazaki *et al.*, 2010, Maggio-Hall *et al.*, 2005, Reverberi *et al.*, 2012, Chen *et al.*, 2018). Dysfunctional peroxisomes have been shown to result in severe and lethal disorders in humans and mammals (Cho *et al.*, 2018, Dixit *et al.*, 2010, Thoms *et al.*, 2009, You *et al.*, 2015). Plant glyoxysomes play essential roles in glyoxylate cycle, embryonic development, and gametophytic function (Hu *et al.*, 2012, Boisson-Dernier *et al.*, 2008). Glycosomes in Trypanosomes perform important glycolytic reactions (Bauer & Morris, 2017). In filamentous fungi, a specific type of peroxisome known as Woronin bodies are associated with septal pore maintenance and cellular integrity (Jedd & Chua, 2000). Recent studies also suggest that peroxisomes play important roles in development, secondary metabolism, and virulence (Kimura *et al.*, 2001, Wang *et al.*, 2013, Soundararajan *et al.*, 2004), but underlying genetic mechanisms associated with these fungal-specific functions still warrant further investigation.

Fusarium verticillioides is a major pathogen of maize, particularly due to ear rot disease and mycotoxin contamination worldwide (Marin *et al.*, 2013, Wu *et al.*, 2014, Woloshuk & Shim, 2013). It is also known as the pathogen responsible for pokkah boeng in sugarcane, and approximately 90% of this disease in China is attributed to *F. verticillioides* (Zhang *et al.*, 2015,

Hilton *et al.*, 2017, Lin *et al.*, 2014). Interestingly, Zhang et al (Zhang *et al.*, 2018b) recently discovered a key peroxisomal matrix protein (FVEG_11334, which is designated as FvPex33 in this study) and a Woronin body associated protein (FvHex1) interacting with Fsr1, a striatin homolog that regulates virulence in *F. verticillioides*. However, gene mutagenesis experiment revealed that FvPex33 and FvHex1 do not directly influence *F. verticillioides* virulence when tested on maize seedlings. This outcome, along with earlier published studies on the role of peroxins in fungal virulence and secondary metabolism (Fujihara *et al.*, 2010, Min *et al.*, 2012, Li *et al.*, 2017) suggested that other peroxisomal matrix proteins may play important roles in *F. verticillioides* virulence and mycotoxin biosynthesis.

Biogenesis of peroxisomes is dynamically regulated in response to environmental and developmental cues (Lazarow, 2003, Heiland & Erdmann, 2005). Metabolic tasks and enzyme content are adjusted according to taxa-specific cellular needs through generation and degradation (Pieuchot & Jedd, 2012, Nuttall *et al.*, 2011). There are two primary pathways for peroxisome formation: *de novo* biogenesis and mature peroxisomes fission. The *de novo* synthesis of peroxisomes has two steps: formation of the peroxisomal membrane and subsequent sorting of peroxisomal matrix proteins to the organelle (Opalinski *et al.*, 2011). The peroxisomal importomer model helps to explain how newly synthesized matrix proteins bind to the cytosolic receptor at the peroxisome membrane and form a highly dynamic pore to transfer matrix proteins to peroxisome lumen (Meinecke *et al.*, 2010). These transient cargo-docking-translocation complexes are formed by variable combination of peroxin (Pex) proteins (Table S1). Briefly, the key docking complex core consists of the SH3-domain protein Pex13 and the PXXP-motif protein Pex14, but also harbors additional factors, e.g. Pex17 in lower eukaryotic cells, Pex33 (also known as Pex14/17) in filamentous fungi, and Pex13.2 in *Trypanosoma brucei* (Verplaetse *et al.*, 2012). A recent study

also characterized Pex17/Pex14/Dyn2p complex in yeast (Chan *et al.*, 2016). Physical association among docking peroxins varies in different organisms, and recent reviews extensively explain how various matrix proteins with type 1 and type 2 peroxisomal targeting signal (PTS1 and PTS2) are recognized by the specific docking complex and associate with the peroxisomal membrane (Nuttall *et al.*, 2011, Pieuchot & Jedd, 2012).

PTS1 and PTS2 peroxisomal matrix proteins are recognized by specific receptors Pex5 and Pex7, respectively, and recruited to the peroxisome docking complex (Meinecke *et al.*, 2010, Heiland & Erdmann, 2005). In addition to these core Peroxins in docking/translocation module (DTM), other Pex proteins are dynamically involved in translocating matrix proteins across the peroxisome membrane (Platta *et al.*, 2013). In particular, Pex8 is known to be associated with DTM but is only present in yeasts and filamentous fungi (Agne *et al.*, 2003). It has been suggested that Pex8 can serve as a importomer-bridging protein to hold the docking complex and the export machinery complex together to facilitate dynamic and transient translocation (Rayapuram & Subramani, 2006, Platta *et al.*, 2013, Meinecke *et al.*, 2010), but the detailed function is largely unknown. In this study, our aim was to characterize putative *F. verticillioides* peroxins, particularly those predicted to be involved in DTM. While paying a close attention to two core components of the docking complex, Pex13 and Pex14, we expanded our study into additional peroxisomal proteins, namely Pex8, that have not been well characterized in plant pathogenic fungi. Through a series of fungal metabolism, physiology and virulence assays, we concluded that Pex8, along with Pex13, plays a critical role in the generation of docking complex in peroxisomes and for peroxisome function in *F. verticillioides* virulence and mycotoxin biosynthesis.

Results

1

2 **Protein-protein interactions between *F. verticillioides* DTM components and other key**
3 **peroxins**

4 Peroxins Pex13 and Pex14 are recognized as key peroxisomal membrane docking complex
5 proteins in eukaryotes, which are required for protein import into peroxisomes. In addition, Pex33
6 has been identified as a new component of the docking complex in *Neurospora crassa* (Managadze
7 *et al.*, 2010), and Pex8 is known to be associated with DTM in yeasts and filamentous fungi (Agne
8 *et al.*, 2003). Using these proteins as query, we screened for putative DTM components, *i.e.* Pex13,
9 Pex14, Pex33, and Pex8, in *F. verticillioides* using the BLASTP algorithm. Additional details for
10 these key Pex proteins, e.g. sequence similarities and putative functional motifs, are provided in
11 Table S1 and Fig. S1A. Notably, further comparison of FvPex33 against Pex14- and Pex17-like
12 proteins in *S. cerevisiae*, *F. graminearum*, *F. verticillioides* strongly suggested that FvPex33 is
13 distinct from Pex14 and Pex17 and is a unique component of DTM in *F. verticillioides* (Fig. S1B).

14 Based on Prediction of Transmembrane Regions and Orientations (TMpred) algorithm
15 (Hoffman and Stoffel, 1993), FvPex8, FvPex13, FvPex14, and FvPex33 are predicted to have
16 transmembrane helices and likely belong to peroxisomes membrane proteins (Fig. S1C). To study
17 the cellular localization of these proteins in *F. verticillioides*, we first chose the biogenesis protein
18 Pex14 as the peroxisomal marker and prepared Pex14-mCherry construct (Grant *et al.*, 2013). We
19 studied transformants containing GFP-fused Pex8, Pex13, or Pex33 protein along with Pex14-
20 mCherry for overlapping red and green fluorescence signals (Fig. 1A), and the images revealed
21 Pex14 co-localizing with Pex13 and Pex33 while showing partial overlap with Pex8.

22 To further verify interactions between key DTM subunits and peroxins, we co-expressed
23 following six pairs of proteins, *i.e.* FvPex13-GFP/FvPex14-mCherry, FvPex13-GFP/FvPex8-

mCherry, FvPex13-GFP/FvPex33-Flag, FvPex33-GFP/FvPex14-mCherry, FvPex8-GFP/FvPex33-Flag, and FvPex8-GFP/FvPex14-mCherry, into *F. verticillioides* for coimmunoprecipitation (Co-IP) experiments. Results showed that FvPex13-GFP successfully associated with the beads and that FvPex14 was eluted in samples that co-expressed FvPex13-GFP and FvPex14-mCherry, indicating FvPex13 and FvPex14 binding *in vivo* (Fig. 1B). Similarly, FvPex13 successfully associated with FvPex8 and FvPex33 (Fig. 1C and D). FvPex33 successfully associated with FvPex14 and FvPex8 (Fig. 1E and F), but FvPex8 did not coprecipitate with FvPex14 (Fig. 1G). We further tested these interactions by yeast two-hybrid assays (Fig. S2A), where FvPex13 showed strong positive interaction with key DTM proteins tested. FvPex8 showed strong interaction with FvPex13 but not with FvPex14. Based on these outcomes, we propose that FvPex13 serves as the core subunit in *F. verticillioides* DTM.

Vegetative growth and conidiation are differentially affected by carbon sources in DTM peroxin mutants

To study the function of key DTM peroxins in *F. verticillioides*, we generated ΔFvpex8, ΔFvpex13, ΔFvpex14, and ΔFvpex33 through targeted gene replacement with the hygromycin-resistance marker in *F. verticillioides* 7600 wild-type strain as described previously (Zhang *et al.*, 2018b). We also generated ΔFvPex33/14 double mutant by replacing *FvPEX14* gene with the geneticin-resistance marker in ΔFvpex33 protoplast. Subsequently, we also generated complementation strains ΔFvpex8-C, ΔFvpex13-C, ΔFvpex14-C, and ΔFvpex33-C by transforming the corresponding mutant with a construct harboring the gene (with its native promoter and terminator) fused with GFP and the geneticin resistance marker. Homologous recombination was confirmed by polymerase chain reaction (PCR) the gene and quantitative PCR

(qPCR) the expression of the gene in corresponding complementation strains (Supplementary Information).

To test whether these mutations impact *F. verticillioides* growth on various carbon nutrients, we cultivated these strains on minium medium (MM) and complete (CMII) agar plates with different carbon sources. On MM agar, we observed varying growth inhibition rates and colony morphologies depending on amended carbon nutrient (Fig. 2A). No strain showed particularly detrimental growth defect on MM, suggesting that these genes are not critical for vegetative growth. But on MM agar with sucrose as the carbon nutrient, vegetative growth and aerial mycelia production in ΔFvpex8 and ΔFvpex33/14 was notably hindered (Fig. 2A and 2B). Inhibition rate was more drastic in ΔFvpex8 on MM agar with butyrate and palmitic acid (Fig. 2A and 2B). Interestingly, aerial mycelium was completely absent in ΔFvpex8 mutant on media with palmitic acid. On CMII agar with sucrose as the carbon source, only ΔFvpex8 exhibted slight growth inhibition but overall all strains were morphologically very similar (Fig. 3SA and 3SB). We also observed a drastic reduction in conidiation in ΔFvpex13 and ΔFvpex33/14 mutants on CMII agar with sucrose (Fig. S3C). However, on CMII with linoleic acid growth inhibition in ΔFvpex8 was more drastic compared to other mutants (Fig. 3SA and 3SB).

Redox homeostasis, cell wall integrity, and lipid degradation in DTM mutants

Peroxisomes serve as one of the primary sources of endogenous and exogenous ROS production. Accumulation of ROS and disruption of redox homeostasis can lead to lower cell survival (Min *et al.*, 2012). When stained with CM-H2DCFDA, mutant hyphae showed green fluorescent granules indicative of high ROS accumulation, especially in ΔFvpex8, ΔFvpex13 and ΔFvpex33/14 mutants (Fig. 3A and 3B). The colonies were stained with 3,3'-diaminobenzidine

1 (DAB) and nitro blue tetrazolium (NBT) for H_2O_2 and O^2- detection, respectively. Yellow and blue
2 colonies were observed in ΔFvpex8, ΔFvpex13, and ΔFvpex33/14 mutants with DAB and NBT
3 staining, respectively (Fig. 3C). Peroxin mutants are likely to display cell wall integrity defects
4 due to their inability to import enzymes of the glyoxylate cycle into peroxisomes (Bhambra et al.
5 2006). Almost all mutants exhibited sensitivity to calcofluor while except for ΔFvpex8 mutant
6 (Fig. 4A). Mutants showed much higher sensitivity in general to sodium dodecyl sulfate (SDS)
7 when compared to the wild type (Fig. 4A). We also observed growth inhibition in DTM mutants
8 on medium amended with H_2O_2 when compared to the WT, which suggested that ability to respond
9 to reactive oxygen species and maintain redox homeostasis was disturbed in these peroxin mutants
10 (Fig. 4A). Growth inhibition rate in peroxin mutants was significantly higher than that of wild type,
11 suggesting DTM peroxins are important for maintaining *F. verticillioides* cell wall integrity (Fig.
12 4B). We also studied lipid droplet degradation and turnover defects in DTM mutants. The mutants
13 accumulated higher levels of lipid droplets compared to WT, particularly when shifted to nutrient
14 starvation (Fig. S4).
15

16 **DTM peroxin FvPex8 function is necessary for FB1 production in *F. verticillioides***

17 *F. verticillioides* is one of the key fungal pathogens responsible for fumonisin
18 contamination of maize worldwide. To assess fumonisin B1 (FB1) accumulation, we
19 independently inoculated B73 maize kernels with spore suspensions of WT, ΔFvpex8, ΔFvpex13,
20 ΔFvpex14, ΔFvpex33, and ΔFvpex33/14 strains. After 10 days of incubation, fungal mass in
21 samples was assessed by qPCR quantification of β-tubulin gene *TUB2* DNA. Fungal mass in
22 ΔFvpex8, ΔFvpex13 and ΔFvpex33/14 mutants was approximately half of those observed in WT,
23 ΔFvpex14, and ΔFvpex33 (Data not shown). When FB1 levels were normalized to fungal mass in

each sample, all mutants showed reduction in FB1 production, ranging from 50% to 94%, with ΔFvpex8 showing the most drastic reduction (Fig. 5A).

To further understand how FvPex8 mutation resulted in such drastic reduction in FB1 biosynthesis, we analyzed transcriptional expression of four key *FUM* genes: polyketide synthase *FUM1*, aminotransferase *FUM8*, transporter *FUM19*, and transcription factor *FUM21* (Bojja *et al.*, 2004, Desjardins & Proctor, 2007, Brown *et al.*, 2007). The expression levels of these genes were assessed by qPCR in WT and ΔFvpex8 strains after a 10-day incubation on corn kernels (Fig. 5B). When compared to the WT, the expression of these four genes were significantly suppressed in ΔFvpex8, particularly *FUM1* showing drastically lower expression levels (Fig. 5B). These outcomes suggest that FvPex8 function is necessary for proper expression of *FUM* genes in *F. verticillioides*, and ultimately fumonisin production.

DTM peroxin FvPex13 plays key roles in *F. verticillioides* virulence

To test whether these DTM Peroxins are associated with virulence, we inoculated B73 maize stalk internodes with spore suspension of the wild-type, ΔFvpex8, ΔFvpex13, ΔFvpex14, ΔFvpex33, and ΔFvpex33/14 strains. When stalks were split open longitudinally after a 10-day incubation, ΔFvpex13 and ΔFvpex33/14 mutants showed drastically reduced rot when compared with the wild-type progenitor and other mutants (Fig. 6A and B). We further tested virulence on sugar cane (cultivar Badila), and outcomes were quite similar to those observed in maize stalk rot assays with ΔFvpex13 showing significantly decreased levels of rot (Fig. S5A and B). It is notable while ΔFvpex14 and ΔFvpex33 single mutations did not impact stalk rot, the double mutant ΔFvpex33/14 showed a significant reduction in virulence when tested on maize and sugarcane stalks. Significantly, ΔFvPex8 mutation did not have any negative impact on *F. verticillioides*

virulence. FvPex13-complemented strain showed wild type-level stalk rot symptoms, suggesting that FvPex13 plays a critical role in *F. verticillioides* virulence on maize and sugarcane.

Deletion of Pex13 impacts cellular localization of DTM peroxins in *F. verticillioides*

A mutation in Pex13 has been linked to PTS1 import defects in yeast, peroxisome abnormalities and appressorium defects in *Colletotrichum orbiculare* (Erdmann & Blobel, 1996, Fujihara *et al.*, 2010). To monitor PTS matrix protein import in *F. verticillioides*, we used confocal microscopy to follow GFP derivatives targeted to the peroxisome. We fused GFP to carnitine O-acetyl transferase gene *FvCAT* containing C-terminal PTS1 sequence (Zolman & Bartel, 2004) or peroxisomal 3-oxoacyl-CoA thiolase gene *FvFOX3* containing *N*-terminal PTS2 sequence (Einerhand *et al.*, 1995) obtaining fusion protein GFP-PTS1 and PTS2-GFP, respectively. We also tested physical interactions between these two PTS proteins and PTS receptor proteins by yeast two-hybrid assays; FvPex5 showed positive results with FvCAT and FvPex7 showed positive results with FvFOX3 (Fig. S2B and C). GFP-PTS1 showed a diffused fluorescence distributed throughout the cytoplasm while PTS2-GFP was restricted to few subcellular organanelles in cytoplasm of 2-days-old ΔFvpex13 hyphae (Fig. 7A). Pex14-mCherry is shown as the peroxisomal marker. These results led us to hypothesize that FvPex13 plays a role in peroxisomal protein targeting via its interaction with FvPex5 and FvPex7. We learned that PTS1 receptor FvPex5 predominantly localizes to the cytoplasm, very similar to FvCat, whereas PTS2 receptor FvPex7 and mPTS receptor FvPex19 are mostly found in cytoplasm in ΔFvpex13 mutant (Fig. 7B). These results suggested that FvPex13 function is not only required to maintain localization but also affect the steady-state size and number levels of these docking peroxins affecting peroxisomes.

1 **Discussion**

2

3 The key aim of this study was to gain a deeper understanding of how peroxisomal
4 docking/translocation module (DTM) complex impacts peroxin import, the integrity and
5 functionality of peroxisomes, and ultimately fumonisin biosynthesis and virulence in maize
6 pathogen *F. verticillioides*. Interaction between four DTM peroxins, *i.e*. FvPex8, FvPex13,
7 FvPex14, and FvPex33, were demonstrated through Co-IP and yeast two-hybrid assays.
8 Interestingly, FvPex8 exhibited no direct interaction with FvPex14. We also confirmed that
9 FvPex14-mCherry colocalizes with FvPex13-GFP, FvPex8-GFP, and FvPex33-GFP in mycelia,
10 suggesting that these proteins form a complex in *F. verticillioides*. FvPex13 plays a more
11 predominant role in PTS1 than PTS2, though FvPex13 is interactive with both PTS receptors. In
12 *S. cerevisiae*, Pex14 preferentially binds to cargo-loaded Pex5 receptor for pore formation while
13 Pex13 is coupled to the translocation of a cargo protein and the close association of Pex13 and
14 Pex14 is required for peroxisomal matrix protein import (Schell-Steven *et al.*, 2005). It was also
15 suggested that Pex13 serves as an initial binding site for the PTS2 pre-import complex, whereas
16 Pex14 assembles with other peroxins in high-molecular-weight complexes after or during
17 dissociation of the PTS2 receptor (Grunau *et al.*, 2009, Meinecke *et al.*, 2010). Based on literature
18 and our experimental data, we envisaged a schematic model of *F. verticillioides* peroxisomal DTM
19 complex shown in Fig. 8. We suggest that FvPex14 and Fvpex33 prefer the initial recognition of
20 the PTS1 cargo-loaded receptor and PTS2 cargo-loaded receptor respectively, while FvPex13 and
21 FvPex8 prefer to unload cargo-loaded from the receptor. Functional role of Pex8 and its association
22 with other key DTM components has not been characterized in fungal pathogens previously.

Recent studies provide numerous examples how key DTM proteins Pex13 and Pex14 are important not only for peroxisome biogenesis but also for hosts of other cellular and physiological functions in filamentous fungi. Absence of the docking peroxin Pex13 in *Podospora anserina* obstructed sexual development prior to meiosis (Suaste-Olmos *et al.*, 2018). *Colletotrichum orbiculare* Pex13 is required for appressorium-mediated plant infection, namely for melanin biosynthesis and turgor generation (Fujihara *et al.*, 2010). Chen and colleagues (2018) showed that Pex13 also plays an important role in *Fusarium graminearum* pathogenesis and mycotoxin biosynthesis. We found very similar outcomes in our study, where *F. verticillioides* Pex13 mediated plant infection and severe peroxisomal defects. Pex14, in addition to its key function as a docking protein, plays a main role in formation of two separate import pores, facilitating the PTS1- and PTS2-dependent protein import into the peroxisomal matrix (Montilla-Martinez *et al.*, 2015, Meinecke *et al.*, 2010). Pex14 has a unique dual function in peroxisome formation and in pexophagy in *Pichia pastoris* and *F. graminearum* (Bellu *et al.*, 2001, Farre *et al.*, 2008, Deng *et al.*, 2013, Lee *et al.*, 2017, Chen *et al.*, 2018). Pex14 serves an important role in Woronin bodies formation in *Neurospora crassa* and host infection in *F. graminearum* (Managadze *et al.*, 2007, Chen *et al.*, 2018). In addition to Pex13 and Pex14, another important component of DTM complex in filamentous fungi is Pex33, a chimeric protein consisting of an N-terminal Pex14-like domain and a C-terminal Pex17-like domain . Pex33 has been associated with glyoxysome biogenesis, sexual and asexual development, virulence and secondary metabolism (Peraza-Reyes *et al.*, 2011, Li *et al.*, 2017, Chen *et al.*, 2018, Opalinski *et al.*, 2010, Managadze *et al.*, 2010). In our study, we found *F. verticillioides* Pex14 and Pex33 collaborate to mediate plant infection and partial peroxisomal defects.

While these key Pex proteins have been extensively investigated in filamentous fungi and other eukaryotes, the role of Pex8 in peroxisomal import machinery and its impact on other physiological roles in pathogenic fungi are still unclear. Pex8, originally discovered as Per1 protein in yeast *Hansenula polymorpha* (syn. *Pichia angusta*), is an intraperoxisomal peroxin that has a PTS1 at the C- terminus and an unusual PTS2 in the mid-protein region (Agne *et al.*, 2003, Waterham *et al.*, 1994). Pex8 is currently the only recognized intraperoxisomal peroxin, while majority of peroxins are either peroxisomal membrane-bound or in the cytosol (Ma *et al.*, 2009, Pieuchot & Jedd, 2012, Girzalsky *et al.*, 2010). Pex8 is targeted to peroxisomes by cytosolic receptors Pex5 (PTS1) or Pex7 (PTS2), and the membrane translocation is primarily mediated through docking complex Pex14 (Agne *et al.*, 2003, Ma *et al.*, 2009). Once positioned in the peroxisomal matrix, Pex8 becomes an important component of importomer complex, anchoring key receptors as well as other membrane-bound peroxins, and serves an important function in both PTS1- and PTS2-dependent protein translocation into peroxisome (Agne *et al.*, 2003, Rehling *et al.*, 2000). Therefore, it is important to acknowledge that composition and organization of the importomer and docking complex can vary in eukaryotes, not only in species-dependent manner but also in a cargo-dependent manner (Gabaldon, 2010, Heiland & Erdmann, 2005, Lazarow, 2003).

In our study, we learned that FvPex8 plays a crucial role in *F. verticillioides* secondary metabolism but is dispensable for plant pathogenesis. Involvement of peroxisomes in fungal secondary metabolite biosynthesis has been well documented, including in penicillin, AK toxin, paxilline, and deoxynivalenol (DON) (Herr & Fischer, 2014, Saikia & Scott, 2009, Imazaki *et al.*, 2010, Martin *et al.*, 2012, Chen *et al.*, 2018). However, it is still unclear how FvPex8 impacts FB1 biosynthetic pathway or regulation. We learned that the expression of key *FUM* genes are

1 decreased drastically in ΔFvpex8 mutant, but it is highly unlikely FvPex8 directly regulates genes
2 in the *FUM* cluster. However, it is possible that Pex8, which contains both peroxisomal targeting
3 signals PTS1 and PTS2, functions as an organizer of the peroxisomal protein import machinery.
4 In *S. cerevisiae*, Pex8 is located at the inner surface of the peroxisomal membrane and is essential
5 for the assembly of the importomer (Deckers *et al.*, 2010). Acetyl-CoA, one of the key buildings
6 block for the synthesis of polyketides, can be produced via various catabolic pathways, including
7 peroxisomal β-oxidation of fatty acids (Maggio-Hall *et al.*, 2005). The FvPex8 mutant showed
8 difficulty growing on multiple carbon sources, raising the hypothesis whether FvPex8 plays a role
9 in peroxisomal carbon recycling and β-oxidation functions. When investigating *F. verticillioides*
10 PTS proteins *in silico*, we also learned that palmitoyl-CoA hydrolase (FVEG_02271, designated
11 FvAct) contains PTS1 and serine palmitoyl transferase (FVEG_12143, designated FvPat) contains
12 PTS2. We can postulate that FvPex8 indirectly impacts hydrolysis of palmitoyl-CoA, which is an
13 acyl-CoA thioester that plays a role in biosynthesis of sphingolipids and in transport of fatty acyl-
14 CoA molecules into the mitochondria for β-oxidation (Brady *et al.*, 1969). Based on current DTM
15 models, inner membrane FvPex8 function may impact both import receptors Pex5 (PTS1 cargo
16 shuttle) and Pex7 (PTS2 cargo shuttle) and disrupt import/export of acetyl-CoA necessary for
17 secondary metabolism in *F. verticillioides*. While we observed higher expression levels of *FvPEX5*
18 and *FvPEX7* when we performed retrograde gene regulation of *FvPEX* genes in ΔFvpex8
19 (Supplementary Information), further study is needed to test this hypothesis.
20 One unexpected outcome in our study was ΔFvpex8 showing no particular defect in virulence.
21 Studies have shown how key peroxisome biogenesis genes are associated with plant infection and
22 pathogenesis in *Colletotrichum lagenarium, C. orbiculare, M. grisea, A. alternata,* and *F.*
23 *graminearum* (Ramos-Pamplona & Naqvi, 2006, Wang *et al.*, 2007, Imazaki *et al.*, 2010, Fujihara

1 *et al.*, 2010, Goh *et al.*, 2011, Min *et al.*, 2012). For instance, CoPex13 is required for appressorium
2 melanization and turgor generation, which are essential for appressorium penetration ability in *C.*
3 *orbiculare* (Fujihara *et al.*, 2010). MoPex33 is required for import of peroxisomal matrix proteins
4 and full virulence in *M. oryzae* (Li *et al.*, 2017). A recent publication described how Pex13, Pex14
5 and Pex33 are critical against host stress agents and pexophagy, ultimately impacting fungal
6 virulence in *F. gramminearum* (Chen *et al.*, 2018). Along with these key DTM components, import
7 receptors Pex5 and Pex7 were also shown to be important for fitness and virulence in fungal
8 pathogens (Min *et al.*, 2012, Wang *et al.*, 2013, Zhang *et al.*, 2018a, Goh *et al.*, 2011). FvPex8
9 showed strong physical interaction with FvPex13, therefore it was reasonable to hypothesize that
10 FvPex8 also plays a critical role in pathogenesis. However, this was not the case; only ΔFvpex13
11 showed impaired virulence in *F. verticillioides* (Fig. 6). FvPex13 is known to affect efficient PTS1
12 and PTS2 imports, and this requires Pex5-Pex13 interaction *in vivo* (Pires *et al.*, 2003, Schell-
13 Steven *et al.*, 2005). Loss of peroxisome function may slow pathogen growth due to inefficient
14 utilization of carbon sources from the host and the fungus itself (Fig. 2 and S3). However, we did
15 not observe similar response in host when challenged by ΔPex8 mutant suggesting that Pex8, while
16 it forms a complex with Pex13 and other DTM components, may not directly contribute to
17 virulence in *F. verticillioides.*
18 To summarize, we identified and characterized *F. verticillioiodes* homologs of DTM
19 components FvPex8, FvPex13, FvPex14, and FvPex33 in this study. Based on our experimental
20 outcomes and literature, we propose a schematic model of core *F. verticillioides* DTM complex
21 (Fig. 8). It is reasonable to hypothesize that these proteins are involved in the regulation of
22 peroxisomal docking complex assembly and matrix translocation and ultimately impact various
23 aspects of fungal development, secondary metabolism, and virulence. However, we clearly noticed

a distinct role each component plays. We propose that the DTM complex plays an important role in virulence through FvPex13, likely in association with FvPex14 and FvPex33. For FB1 production, FvPex8 was determined as the key components, but the mechanism in which FvPex8 regulates FB1 biosynthesis needs further investigation.

Material and methods

Fungal strains and culture media

F. verticillioides wild-type strain 7600 and all transformants (Table S2) were cultured on complete medium (CMII: 2% sucrose, 0.05% magnesium sulfate heptahydrate, 0.1% potassium dihydrogen phosphate, 0.05% potassium chloride, 0.2% nitrate potassium acid, 0.1% hydrolyzed casein, 0.2% peptone, 0.1% Wolfe's Vitamin Solution [Coolaber, China], 1.8% agar) and minimal medium (MM) (Leslie & Summerell, 2006). CMII agar with 250 µg/ml hygromycin B (Roche, Germany), 200 µg/ml G418 (Sigma, USA) or 800 µg/ml G418 (Sigma) were used for screening transformants. For conidia production assay, six 0.7 cm- diameter agar blocks were added to 3 ml water, vortexed and conidia were quantified by a hemocytometer. For vegetative growth and stress agent sensitivity assays, the wild-type and mutant strains were grown on MM and CMII amended with various carbon sources: potassium acetate (40 mM), sodium butyrate (10 mM), sucrose (2%), palmitic acid (3 mM), oleic acid (3 mM) or linoleic acid (3 mM) (Min *et al.*, 2012). Colony diameter was measured after 5 days of incubation. Cell wall integrity was tested by growing the strains on CMII supplemented with 200mg/ml Calcofluor white (CFW) or 0.01% sodium dodecyl sulfate (SDS). The tolerance of strains to exogenous ROS was evaluated by measuring growth on CMII containing 0.05% H_2O_2.

1

2 **Generation of the DTM gene deletion mutants and GFP/mCherry/Flag-tagged strains**

3 Single DTM gene *F. verticillioides* mutants were generated with a split-marker approach
4 described previously (Zhang *et al.*, 2018b). All primers used in this study are listed in Table S3.
5 For double deletion of *FvPEX14* and *FvPEX33*, we replaced the *FvPEX14* with neomycin
6 phosphotransferase (*NEO*) gene in the ΔFvpex33 deletion mutant. Protoplasts were generated,
7 transformed and screened following our standard PCR and qPCR (Yan & Shim, 2020, Zhang *et*
8 *al.*, 2018b). For qPCR, the wild-type and DTM mutants were inoculated in CMII medium for 3
9 days. The extraction of total RNA and the synthesis of first-strand cDNA were performed as
10 previously described (Yan & Shim, 2020). The expression of peroxins, were detected by qRT-
11 PCR using SuperReal PreMix Plus (SYBR Green) (Tiangen Biotech, China). As an endogenous
12 control, a 200-bp amplicon of *F. verticillioides* β-tubulin (*TUB2*) gene (FVEG_04081) was
13 amplified, and the relative quantification of each transcript was calculated following the standard
14 $2^{-\Delta\Delta CT}$ method (Yan & Shim, 2020). Primers used to amplify selected genes in qPCR reactions are
15 listed in Table S3. All qPCR assays were conducted in triplicates for each sample and the
16 experiment was repeated three times. Subsequently, we constructed the fusion GFP and mCherry
17 vectors following the protocol described previously (Zhang *et al.*, 2018b, Yan & Shim, 2020). All
18 fusion vectors generated were sequenced before transformation. For construction of GFP-tagged
19 strains, we transformed corresponding fusion GFP vectors with G418 sulfate-resistant (*GEN*) gene
20 into protoplasts. For testing whether FvPex13 affected the localization of PTS pathway related
21 genes, we transformed fusion GFP vectors with *GEN* into WT and ΔFvPex13 mutant protoplasts.
22 For testing whether FvPex33 interacts with other DTM, we transformed Flag vectors and fusion
23 Flag-FvPex33 with *GEN* into WT and ΔFvPex33 mutant protoplasts, respectively.

1

2

3 **ROS and lipid staining and quantification**

4 For lipid staining, 2-day-old mycelia were harvested as 0h, and corresponding 2-day-old
5 mycelia were transfered to PBS medium for 18 h , washing mycelia twice with water. Hypha was
6 tested by staining with Nile Red on 0h and 18 h respectivly (Nguyen *et al.*, 2011). Cellular ROS
7 accumulation in the fungal hyphae was analyzed using the CM-H2DCFDA staining. Mycelia were
8 harvested and washed with PBS for 3 times. Hypha was stained with CM-H2DCFDA (5 μM)
9 (Sigma) for 10 min in the dark following GENMED reagent protocols, scanning confocal
10 microscope with excitation at 490nm (GENMED Scientifics, USA). Accumulation of ROS in
11 mycelia was visualized with 6-chloromethyl-2',7'-dichlorodihydrofluorescein diacetate (CM-
12 H2DCFDA) staining. Endogenous ROS scavenging capacity was tested by growing the strains on
13 CMII medium 5 days, and the colony were stained with 3,3'-diaminobenzidine (DAB) for H_2O_2
14 detection and with 2mM Nitro Blue Tetrazolium (NBT) (Sigma) in 20mM phosphate buffer, pH6
15 for O^{2-} detection treated, respectively.

16

17 **Co-immunoprecipitation and yeast two-hybrid assays**

18 Strains were grown in CMII medium for 2 days before immunoblot and immunoprecipitation
19 analyses were conducted as previously described (Zheng *et al.*, 2015). For total protein extraction,
20 mycelia of FvPex13-GFP and FvPex14-mCherry were ground into a fine powder in liquid nitrogen
21 and resuspended in 30-mL extraction buffer (10 mM Tris/Cl pH 7.5, 150 mM NaCl, 0.5 mM EDTA,
22 0.5% NP40, 1 mM PMSF). The supernatants were centrifuged 15,000 g for 25 min at 4°C to
23 remove cell debris. For immunoprecipitation of GFP-fusion proteins from cellular extracts, equal

concentration of total proteins was isolated and incubated with 20~30 μL of GFP-Trap agarose beads (ChromoTek, Germany) according to manufacturer's instructions. Proteins eluted from GFP-Trap agarose beads were analyzed by immunoblot detection with the anti-mCherry, anti-Flag (Clontech, USA) and anti-GFP (Sigma) antibodies.

The yeast two-hybrid assay was carried out following our previous standard protocol (Zhang *et al.*, 2018b). The coding sequence of each tested gene was amplified from wild-type cDNA. *FvPEX13* and *FvPEX14* were cloned into pGBKT7 as the bait vectors. Other components of the DTM *FvPEX8*, *FvPEX14*, *FvPEX33*, along with *FvPEX5* and *FvPEX7* cDNA were amplified and cloned into pGADT7 as the prey vectors. The pairs of plasmids pGBKT7-P53 and pGADT7-T, pGBKT7-Lam and pGADT7-T were used as the positive and the negative control, respectively. All primers used in this study were listed in Table S3. Further details are provided in Supplementary Information.

Virulence and FB1 assays

Infection assays on maize and sugarcane stalks were conducted as previously described (Zhang *et al.*, 2018b, Zhang *et al.*, 2015). Subsequently, maize and sugar cane stalks were split longitudinally to assess disease severity and to quantify the extent of the rot by Image J software. For FB1 assay, conidia were inoculated on surface sterilized B73 corn kernel for 10 days and quantified with Fumonisin B1 ELISA Kit following manufacturer's suggested protocol (Biovision, USA). FB1 concentrations were obtained by the optical density (OD value) of each well at 450 nm with a microplate reader by comparing to FB1 standard curve. *F. verticillioides* biomass quantification was calculated by qPCR based on the *TUB*2 standard curve, which was measured at 0.01, 0.1, 1.0, 10 ng/μl concentrations (Rocha *et al.*, 2015). Sample FB1 levels were normalized

by calculating FB1 ppm/ *TUB*2 DNA concentration. To compare the *FUM* gene expression, RNA samples were prepared from ΔFvpex8 mutant and *F. verticillioides* strains grown on corn kernel for 10 days. The expression levels of *FUM1*, *FUM8*, *FUM19* and *FUM21* were normalized to *TUB2* expression. The experiment was repeated three times.

Author Contributions

W.Y., W-B.S. and Z.W. conceived and designed the experiments. W.Y., M.L., H.Y. and Y.H. performed the experiments. W.Y., J.Z., G.L., W-B.S. and Z.W analyzed the data. W.Y., H.Y., W-B.S. and Z.W. wrote the paper.

Acknowledgments

This work was supported by the NSFC grants (#31601599) and Science and Technology Innovation Special Fund of FAFU(#CXZX2017138). The authors declare no conflict of interest.

References

Agne, B., Meindl, N. M., Niederhoff, K., Einwachter, H., Rehling, P., Sickmann, A., Meyer, H. E., Girzalsky, W. and Kunau, W. H. (2003) Pex8p: An intraperioxisomal organizer of the peroxisomal import machinery. *Mol Cell,* **11,** 635-646.

Alberts, B., Johnson, A., Lewis, J., Raff, M., Roberts, K. and Walter, P. (2002) Peroxisomes. In: *Mol Biol Cell.* New York: Garland Science.

Bauer, S. and Morris, M. T. (2017) Glycosome biogenesis in trypanosomes and the *de novo* dilemma. *Plos Neglect Trop D,* **11,** e0005333.

Bellu, A. R., Komori, M., van der Klei, I. J., Kiel, J. A. and Veenhuis, M. (2001) Peroxisome biogenesis and selective degradation converge at Pex14p. *J Biol Chem,* **276,** 44570-44574.

Boisson-Dernier, A., Frietsch, S., Kim, T. H., Dizon, M. B. and Schroeder, J. I. (2008) The peroxin loss-of-function mutation abstinence by mutual consent disrupts male-female gametophyte recognition. *Curr Biol,* **18,** 63-68.

Bojja, R. S., Cerny, R. L., Proctor, R. H. and Du, L. (2004) Determining the biosynthetic sequence in the early steps of the fumonisin pathway by use of three gene-disruption mutants of *Fusarium verticillioides*. *J Agric Food Chem,* **52,** 2855-2860.

Brady, R. N., Di Mari, S. J. and Snell, E. E. (1969) Biosynthesis of sphingolipid bases. 3. Isolation and characterization of ketonic intermediates in the synthesis of sphingosine and dihydrosphingosine by cell-free extracts of *Hansenula ciferri*. *J Biol Chem,* **244,** 491-496.

Brown, D. W., Butchko, R. A., Busman, M. and Proctor, R. H. (2007) The *Fusarium verticillioides FUM* gene cluster encodes a Zn(II)2Cys6 protein that affects *FUM* gene expression and fumonisin production. *Eukaryotic Cell,* **6,** 1210-1218.

Chan, A., Schummer, A., Fischer, S., Schroter, T., Cruz-Zaragoza, L. D., Bender, J., Drepper, F., Oeljeklaus, S., Kunau, W. H., Girzalsky, W., Warscheid, B. and Erdmann, R. (2016) Pex17p-dependent assembly of Pex14p/Dyn2p-subcomplexes of the peroxisomal protein import machinery. *Eur J Cell Biol,* **95,** 585-597.

Chen, Y., Zheng, S., Ju, Z., Zhang, C., Tang, G., Wang, J., Wen, Z., Chen, W. and Ma, Z. (2018) Contribution of peroxisomal docking machinery to mycotoxin biosynthesis, pathogenicity and pexophagy in the plant pathogenic fungus *Fusarium graminearum*. *Environmental Microbiology,* **20,** 3224-3245.

Cho, D. H., Kim, Y. S., Jo, D. S., Choe, S. K. and Jo, E. K. (2018) Pexophagy: Molecular Mechanisms and Implications for Health and Diseases. *Mol Cells,* **41,** 55-64.

Cooper, G. M. (2000) Bioenergetics and Metabolism - Mitochondria, Chloroplasts, and Peroxisomes. In: *The Cell: A Molecular Approach.* Sunderland, MA: Sinauer Associates.

Deckers, M., Emmrich, K., Girzalsky, W., Awa, W. L., Kunau, W. H. and Erdmann, R. (2010) Targeting of Pex8p to the peroxisomal importomer. *Eur J Cell Biol,* **89,** 924-931.

Deng, Y., Qu, Z. and Naqvi, N. I. (2013) The role of snx41-based pexophagy in *Magnaporthe* development. *PLoS One,* **8,** e79128.

Desjardins, A. E. and Proctor, R. H. (2007) Molecular biology of Fusarium mycotoxins. *Int J Food Microbiol,* **119,** 47-50.

Dixit, E., Boulant, S., Zhang, Y., Lee, A. S., Odendall, C., Shum, B., Hacohen, N., Chen, Z. J., Whelan, S. P., Fransen, M., Nibert, M. L., Superti-Furga, G. and Kagan, J. C. (2010) Peroxisomes are signaling platforms for antiviral innate immunity. *Cell,* **141,** 668-681.

Einerhand, A. W. C., Kos, W., Smart, W. C., Kal, A. J., Tabak, H. F. and Cooper, T. G. (1995) The upstream region of the Fox3 gene encoding peroxisomal 3-oxoacyl-coenzyme-A thiolase in *Saccharomyces cerevisiae* contains Abf1-binding and replication protein-A-binding sites that participate in its regulation by glucose repression. *Mol Cell Biol,* **15,** 3405-3414.

Erdmann, R. and Blobel, G. (1996) Identification of Pex13p a peroxisomal membrane receptor for the PTS1 recognition factor. *J Cell Biol,* **135,** 111-121.

Farre, J. C., Manjithaya, R., Mathewson, R. D. and Subramani, S. (2008) PpAtg30 tags peroxisomes for turnover by selective autophagy. *Dev Cell,* **14,** 365-376.

Fujihara, N., Sakaguchi, A., Tanaka, S., Fujii, S., Tsuji, G., Shiraishi, T., O'Connell, R. and Kubo, Y. (2010) Peroxisome biogenesis factor *PEX13* is required for appressorium-mediated plant infection by the anthracnose fungus *Colletotrichum orbiculare*. *Mol Plant Microbe Interact,* **23,** 436-445.

Gabaldon, T. (2010) Peroxisome diversity and evolution. *Philos Trans R Soc Lond B Biol Sci,* **365,** 765-773.

Girzalsky, W., Saffian, D. and Erdmann, R. (2010) Peroxisomal protein translocation. *BBA - Mol Cell Res,* **1803,** 724-731.

Goh, J., Jeon, J., Kim, K. S., Park, J., Park, S. Y. and Lee, Y. H. (2011) The *PEX7*-mediated peroxisomal import system is required for fungal development and pathogenicity in *Magnaporthe oryzae*. *PLoS One,* **6,** e28220.

Grant, P., Ahlemeyer, B., Karnati, S., Berg, T., Stelzig, I., Nenicu, A., Kuchelmeister, K., Crane, D. I. and Baumgart-Vogt, E. (2013) The biogenesis protein PEX14 is an optimal marker for the identification and localization of peroxisomes in different cell types, tissues, and species in morphological studies. *Histochem Cell Biol,* **140,** 423-442.

Grunau, S., Schliebs, W., Linnepe, R., Neufeld, C., Cizmowski, C., Reinartz, B., Meyer, H. E., Warscheid, B., Girzalsky, W. and Erdmann, R. (2009) Peroxisomal targeting of PTS2 pre-import complexes in the yeast *Saccharomyces cerevisiae*. *Traffic,* **10,** 451-460.

Heiland, I. and Erdmann, R. (2005) Biogenesis of peroxisomes - Topogenesis of the peroxisomal membrane and matrix proteins. *Febs J,* **272,** 2362-2372.

Herr, A. and Fischer, R. (2014) Improvement of *Aspergillus nidulans* penicillin production by targeting AcvA to peroxisomes. *Metab Eng,* **25,** 131-139.

Hilton, A., Zhang, H. M., Yu, W. Y. and Shim, W. B. (2017) Identification and characterization of pathogenic and endophytic fungal species associated with Pokkah Boeng disease of sugarcane. *Plant Pathology J,* **33,** 238-248.

Hu, J., Baker, A., Bartel, B., Linka, N., Mullen, R. T., Reumann, S. and Zolman, B. K. (2012) Plant peroxisomes: biogenesis and function. *Plant Cell,* **24,** 2279-2303.

Imazaki, A., Tanaka, A., Harimoto, Y., Yamamoto, M., Akimitsu, K., Park, P. and Tsuge, T. (2010) Contribution of peroxisomes to secondary metabolism and pathogenicity in the fungal plant pathogen *Alternaria alternata*. *Eukaryot Cell,* **9,** 682-694.

Jedd, G. and Chua, N. H. (2000) A new self-assembled peroxisomal vesicle required for efficient resealing of the plasma membrane. *Nat Cell Biol,* **2,** 226-231.

Kimura, A., Takano, Y., Furusawa, I. and Okuno, T. (2001) Peroxisomal metabolic function is required for appressorium-mediated plant infection by *Colletotrichum lagenarium*. *Plant Cell,* **13,** 1945-1957.

Lazarow, P. B. (2003) Peroxisome biogenesis: advances and conundrums. *Curr Opin Cell Biol,* **15,** 489-497.

Lee, M. Y., Sumpter, R., Jr., Zou, Z., Sirasanagandla, S., Wei, Y., Mishra, P., Rosewich, H., Crane, D. I. and Levine, B. (2017) Peroxisomal protein PEX13 functions in selective autophagy. *EMBO Rep,* **18,** 48-60.

Leslie, J. F. and Summerell, B. A. (2006) *The Fusarium Laboratory Manual*. Ames, Iowa: Blackwell Publishing.

Li, L., Wang, J., Chen, H., Chai, R., Zhang, Z., Mao, X., Qiu, H., Jiang, H., Wang, Y. and Sun, G. (2017) Pex14/17, a filamentous fungus-specific peroxin, is required for the import of peroxisomal matrix proteins and full virulence of *Magnaporthe oryzae*. *Mol Plant Pathol,* **18,** 1238-1252.

Lin, Z. Y., Xu, S. Q., Que, Y. X., Wang, J. H., Comstock, J. C., Wei, J. J., McCord, P. H., Chen, B. S., Chen, R. K. and Zhang, M. Q. (2014) Species-specific detection and identification of *Fusarium* species complex, the causal agent of sugarcane Pokkah Boeng in China. *PLoS One,* **9**.

Ma, C., Schumann, U., Rayapuram, N. and Subramani, S. (2009) The peroxisomal matrix import of Pex8p requires only PTS receptors and Pex14p. *Mol Biol Cell,* **20,** 3680-3689.

Maggio-Hall, L. A., Wilson, R. A. and Keller, N. P. (2005) Fundamental contribution of beta-oxidation to polyketide mycotoxin production in planta. *Mol Plant Microbe Interact,* **18,** 783-793.

Managadze, D., Wurtz, C., Sichting, M., Niehaus, G., Veenhuis, M. and Rottensteiner, H. (2007) The peroxin PEX14 of *Neurospora crassa* is essential for the biogenesis of both glyoxysomes and Woronin bodies. *Traffic,* **8,** 687-701.

Managadze, D., Wurtz, C., Wiese, S., Schneider, M., Girzalsky, W., Meyer, H. E., Erdmann, R., Warscheid, B. and Rottensteiner, H. (2010) Identification of PEX33, a novel component of the peroxisomal docking complex in the filamentous fungus *Neurospora crassa*. *Eur J Cell Biol,* **89,** 955-964.

Marin, S., Ramos, A. J., Cano-Sancho, G. and Sanchis, V. (2013) Mycotoxins: Occurrence, toxicology, and exposure assessment. *Food Chem Toxicol,* **60,** 218-237.

Martin, J. F., Ullan, R. V. and Garcia-Estrada, C. (2012) Role of peroxisomes in the biosynthesis and secretion of beta-lactams and other secondary metabolites. *J Ind Microbiol Biotechnol,* **39,** 367-382.

Meinecke, M., Cizmowski, C., Schliebs, W., Kruger, V., Beck, S., Wagner, R. and Erdmann, R. (2010) The peroxisomal importomer constitutes a large and highly dynamic pore. *Nat Cell Biol,* **12,** 273-277.

Min, K., Son, H., Lee, J., Choi, G. J., Kim, J. C. and Lee, Y. W. (2012) Peroxisome function is required for virulence and survival of *Fusarium graminearum*. *Mol Plant Microbe Interact,* **25,** 1617-1627.

Montilla-Martinez, M., Beck, S., Klumper, J., Meinecke, M., Schliebs, W., Wagner, R. and Erdmann, R. (2015) Distinct pores for peroxisomal import of PTS1 and PTS2 proteins. *Cell Rep,* **13,** 2126-2134.

Nguyen, L. N., Bormann, J., Le, G. T., Starkel, C., Olsson, S., Nosanchuk, J. D., Giese, H. and Schafer, W. (2011) Autophagy-related lipase FgATG15 of *Fusarium graminearum* is important for lipid turnover and plant infection. *Fungal Genet Biol,* **48,** 217-224.

Nuttall, J. M., Motley, A. and Hettema, E. H. (2011) Peroxisome biogenesis: recent advances. *Curr Opin Cell Biol,* **23,** 421-426.

Opalinski, L., Kiel, J. A., Homan, T. G., Veenhuis, M. and van der Klei, I. J. (2010) *Penicillium chrysogenum* Pex14/17p--a novel component of the peroxisomal membrane that is important for penicillin production. *Febs J,* **277,** 3203-3218.

Opalinski, L., Kiel, J. A. K. W., Williams, C., Veenhuis, M. and van der Klei, I. J. (2011) Membrane curvature during peroxisome fission requires Pex11. *Embo J,* **30,** 5-16.

Peraza-Reyes, L., Arnaise, S., Zickler, D., Coppin, E., Debuchy, R. and Berteaux-Lecellier, V. (2011) The importomer peroxins are differentially required for peroxisome assembly and meiotic development in *Podospora anserina*: insights into a new peroxisome import pathway. *Mol Microbiol,* **82,** 365-377.

Pieuchot, L. and Jedd, G. (2012) Peroxisome assembly and functional diversity in eukaryotic microorganisms. *Annual Review of Microbiology,* **66,** 237-263.

Pires, J. R., Hong, X., Brockmann, C., Volkmer-Engert, R., Schneider-Mergener, J., Oschkinat, H. and Erdmann, R. (2003) The ScPex13p SH3 domain exposes two distinct binding sites for Pex5p and Pex14p. *J Mol Biol,* **326,** 1427-1435.

Platta, H. W., Hagen, S. and Erdmann, R. (2013) The exportomer: the peroxisomal receptor export machinery. *Cell Mol Life Sci,* **70,** 1393-1411.

Ramos-Pamplona, M. and Naqvi, N. I. (2006) Host invasion during rice-blast disease requires carnitine-dependent transport of peroxisomal acetyl-CoA. *Mol Microbiol,* **61,** 61-75.

Rayapuram, N. and Subramani, S. (2006) The importomer - A peroxisomal membrane complex involved in protein translocation into the peroxisome matrix. *BBA - Mol Cell Res,* **1763,** 1613-1619.

Rehling, P., Skaletz-Rorowski, A., Girzalsky, W., Voorn-Brouwer, T., Franse, M. M., Distel, B., Veenhuis, M., Kunau, W. H. and Erdmann, R. (2000) Pex8p, an intraperoxisomal peroxin of *Saccharomyces cerevisiae* required for protein transport into peroxisomes binds the PTS1 receptor Pex5p. *Journal of Biological Chemistry,* **275,** 3593-3602.

Reverberi, M., Punelli, M., Smith, C. A., Zjalic, S., Scarpari, M., Scala, V., Cardinali, G., Aspite, N., Pinzari, F., Payne, G. A., Fabbri, A. A. and Fanelli, C. (2012) How peroxisomes affect aflatoxin biosynthesis in *Aspergillus flavus*. *PLoS One,* **7,** e48097.

Rocha, L. O., Barroso, V. M., Andrade, L. J., Pereira, G. H., Ferreira-Castro, F. L., Duarte, A. P., Michelotto, M. D. and Correa, B. (2015) *FUM* gene expression profile and fumonisin production by *Fusarium verticillioides* inoculated in Bt and non-Bt maize. *Front Microbiol,* **6,** 1503.

Saikia, S. and Scott, B. (2009) Functional analysis and subcellular localization of two geranylgeranyl diphosphate synthases from *Penicillium paxilli*. *Mol Genet Genomics,* **282,** 257-271.

Schell-Steven, A., Stein, K., Amoros, M., Landgraf, C., Volkmer-Engert, R., Rottensteiner, H. and Erdmann, R. (2005) Identification of a novel, intraperoxisomal pex14-binding site in pex13: association of pex13 with the docking complex is essential for peroxisomal matrix protein import. *Mol Cell Biol,* **25,** 3007-3018.

Soundararajan, S., Jedd, G., Li, X., Ramos-Pamplona, M., Chua, N. H. and Naqvi, N. I. (2004) Woronin body function in *Magnaporthe grisea* is essential for efficient pathogenesis and for survival during nitrogen starvation stress. *Plant Cell,* **16,** 1564-1574.

Suaste-Olmos, F., Zirion-Martinez, C., Takano-Rojas, H. and Peraza-Reyes, L. (2018) Meiotic development initiation in the fungus *Podospora anserina* requires the peroxisome receptor export machinery. *Biochim et Biophys Acta - Mol Cell Res,* **1865,** 572-586.

Thoms, S., Gronborg, S. and Gartner, J. (2009) Organelle interplay in peroxisomal disorders. *Trends Mol Med,* **15,** 293-302.

Verplaetse, E., Gualdron-Lopez, M., Chevalier, N. and Michels, P. A. M. (2012) Studies on the organization of the docking complex involved in matrix protein import into glycosomes of *Trypanosoma brucei*. *Biochem Bioph Res Co,* **424,** 781-785.

Wang, J., Zhang, Z., Wang, Y., Li, L., Chai, R., Mao, X., Jiang, H., Qiu, H., Du, X., Lin, F. and Sun, G. (2013) PTS1 peroxisomal import pathway plays shared and distinct roles to PTS2 pathway in development and pathogenicity of *Magnaporthe oryzae*. *PLoS One,* **8,** e55554.

Wang, Z. Y., Soanes, D. M., Kershaw, M. J. and Talbot, N. J. (2007) Functional analysis of lipid metabolism in *Magnaporthe grisea* reveals a requirement for peroxisomal fatty acid beta-oxidation during appressorium-mediated plant infection. *Mol Plant Microbe Interact,* **20,** 475-491.

Waterham, H. R., Titorenko, V. I., Haima, P., Cregg, J. M., Harder, W. and Veenhuis, M. (1994) The *Hansenula polymorpha* Per1 gene is essential for peroxisome biogenesis and encodes a peroxisomal matrix protein with both carboxy-terminal and amino-terminal targeting signals. *Journal of Cell Biology,* **127,** 737-749.

Woloshuk, C. P. and Shim, W. B. (2013) Aflatoxins, fumonisins, and trichothecenes: a convergence of knowledge. *Fems Microbiol Rev,* **37,** 94-109.

Wu, F., Groopman, J. D. and Pestka, J. J. (2014) Public Health Impacts of Foodborne Mycotoxins. *Annual Review of Food Science and Technology,* **5,** 351-372.

Yan, H. and Shim, W. B. (2020) Characterization of non-canonical G beta-like protein FvGbb2 and its relationship with heterotrimeric G proteins in *Fusarium verticillioides*. *Environ Microbiol,* **22,** 615-628.

You, J., Hou, S., Malik-Soni, N., Xu, Z., Kumar, A., Rachubinski, R. A., Frappier, L. and Hobman, T. C. (2015) Flavivirus infection impairs peroxisome biogenesis and early antiviral signaling. *J Virol,* **89,** 12349-12361.

Zhang, C. K., Wang, J. Q., Tao, H., Dang, X., Wang, Y., Chen, M. P., Zhai, Z. Z., Yu, W. Y., Xu, L. P., Shim, W. B., Lu, G. D. and Wang, Z. H. (2015) FvBck1, a component of cell wall integrity MAP kinase pathway, is required for virulence and oxidative stress response in sugarcane Pokkah Boeng pathogen. *Front Microbiol,* **6,** 1096.

Zhang, F., Geng, L., Huang, L., Deng, J., Fasoyin, O. E., Yao, G. and Wang, S. (2018a) Contribution of peroxisomal protein importer AflPex5 to development and pathogenesis in the fungus *Aspergillus flavus*. *Curr Genet,* **64,** 1335-1348.

Zhang, H., Mukherjee, M., Kim, J. E., Yu, W. and Shim, W. B. (2018b) Fsr1, a striatin homologue, forms an endomembrane-associated complex that regulates virulence in the maize pathogen *Fusarium verticillioides*. *Mol Plant Pathol,* **19,** 812-826.

Zheng, W., Zhou, J., He, Y., Xie, Q., Chen, A., Zheng, H., Shi, L., Zhao, X., Zhang, C., Huang, Q., Fang, K., Lu, G., Ebbole, D. J., Li, G., Naqvi, N. I. and Wang, Z. (2015) Retromer is essential for autophagy-dependent plant infection by the rice blast fungus. *PLoS Genet,* **11,** e1005704.

Zolman, B. K. and Bartel, B. (2004) An Arabidopsis indole-3-butyric acid-response mutant defective in PEROXIN6, an apparent ATPase implicated in peroxisomal function. *P Natl Acad Sci USA,* **101,** 1786-1791.

1 **Figure legends**

2

3 **Fig. 1. FvPex8, FvPex13, FvPex14, and FvPex33 protein interaction analyses.**

4 (A) Localization of FvPex8-GFP, FvPex13-GFP, and FvPex33-GFP were studied in comparison
5 to FvPex14-mCherry, which was used as a peroxisomal marker, in the wild-type strain. Scale bar
6 = 10 μm. GFP-trap-based pull-down experiment showing the interaction *in vitro* between (B)
7 FvPex13 and FvPex14, (C) FvPex13 and FvPex8, (D) FvPex33 and FvPex13, (E) FvPex33 and
8 FvPex14, (F) FvPex33 and FvPex8, and (G) FvPex8 and FvPex14. The strains co-expressing the
9 indicated proteins were immunoprecipitated with GFP trap beads. The IP signal (FvPex13-GFP,
10 FvPex8-GFP, or FvPex33-GFP) and the Co-IP signal (FvPex8-mCherry, FvPex14-mCherry, or
11 FvPex33-Flag) were detected by immunoblots probed with antibodies to GFP, mCherry, and Flag,
12 respectively.

13

14 **Fig. 2. Impact of FvPex8 on *PEX* gene transcription and carbon source utilization.**

15 (A) Vegetative growth and aerial mycelia production in wild-type (WT) and mutant strains were
16 monitored on minimal medium (MM) amended with different carbon sources. Colony morphology
17 was photographed after 5 days of incubation at 25°C. (B) The growth inhibition rate was analyzed
18 by comparing the growth of wild type with mutants on MM agar with various carbon amendments.
19 The mycelial growth inhibition rate (%) was measured by [(the diameter of WT strain - the
20 diameter of mutant strain)/(the diameter of WT strain)]×100%). Bar indicates the standard
21 deviation of three replicates. An asterisk above the column indicates a statistically significant
22 difference ($P<0.05$) as anlyzed by t-test.

23

1 **Fig. 3. Reactive oxygen species response in mutants**

2 (A) Fungal hyphae were grown for 2 days and stained with CM-H2DCFDA to measure cellular
3 ROS accumulation in wild-type strain Fv7600 and mutants. Accumulation of ROS in mycelia was
4 visualized with 6-chloromethyl-2',7'-dichlorodihydrofluorescein diacetate (CM-H2DCFDA)
5 staining. Scale bar = 10 μm. (B) ROS accumulation was quantified by Image J software. Error bars
6 represent the deviation from three replicates and an asterisk above the column indicates a
7 statistically significant difference ($P<0.05$) as anlyzed by t-test. (C) Endogenous ROS scavenging
8 capacity was tested by staining fungal strains grown on CMII medium for 5 days with 3,3'-
9 diaminobenzidine (DAB) for H_2O_2 detection and with Nitro Blue Tetrazolium (NBT) for O^{2-}
10 detection.

11

12 **Fig. 4. Disruption of peroxisomal functions promotes reactive oxygen species (ROS)**
13 **accumulation**.

14 (A) Mycelial growth of the wild type (WT) and mutants was monitored on CMII media
15 supplemented with sodium dodecyl sulfate (SDS), Calcofluor white (CFW), and H_2O_2 for 5 days.
16 Plates were photographed after 5 days of incubation at 25°C. (B) Mycelial growth inhibition rates
17 were calculated by [(the diameter of WT strain - the diameter of mutant strain)/(the diameter of
18 WT strain)]×100%. An asterisk above the column indicates a statistically significant difference
19 ($P<0.05$) as anlyzed by t-test.

20

21 **Fig. 5. Role of peroxins in fumonisin B1 (FB1) production and *FUM* gene expression**

22 (A) Surface sterilized B73 corn kernels were inoculated with wild type (WT) and mutant fungal
23 conidia and were incubated for 10 days before FB1 levels were quantified by ELISA Kit. *F.*

1 *verticillioides* biomass was quantified by measuring *F. verticillioides* β-tubulin (*TUB2*) DNA in
2 samples. FB1 level in samples was normalized by calculating FB1 (ppm)/ *TUB2* DNA (ng). (B)
3 To compare the expression levels of key *FUM* genes, RNA samples were prepared from the wild
4 type (WT) and ΔFvpex8 mutant on corn kernel for 10 days. The expression levels of *FUM1*, *FUM8*,
5 *FUM19* and *FUM21* were normalized to *TUB2* expression. The experiment was repeated three
6 times, and error bars represent the standard deviation from three replicates. An asterisk above the
7 column indicates a statistically significant difference (P<0.05) as anlyzed by t-test.
8
9 **Fig. 6. Role of DTM peroxins in maize stalk rot virulence.**
10 (A) Maize B73 stalks were inoculated with wild type (WT) and mutant fungal spore suspension
11 (10^6/ml) at the internodal region and incubated at room temperature for 7 days. Subsequently,
12 maize stalks were split longitudinally to visually inspect rot symptoms. (B) Image J software was
13 used to quantify the extent of the rot in each sample. Three independent biological repetitions were
14 performed and error bars represent the standard deviation from three replicates. An asterisk above
15 the column indicates a statistically significant difference (P<0.05) as anlyzed by t-test. Sterile
16 water was used as a negative control (Fig. S5).
17
18 **Fig.7. Fvpex13 plays an important role in mycelial peroxin localization.**
19 (A) GFP fused to C-terminal PTS1 sequence (PTS1-GFP) and N-terminal PTS2 sequence (GFP-
20 PTS2), localizations were studied in the wild type (WT) and ΔFvpex13 mutant. Pex14-mCherry
21 signal was used as the peroxisomal marker. Bars = 2 μm. (B) Localization of key DTM peroxins
22 Pex8, Pex7, Pex19, and Pex5 were studied in the wild type (WT) and ΔFvpex13 mutant. Pex14

was monitored in ΔFvpex14 and ΔFvpex13, while Pex33-GFP was monitored in ΔFvpex33 and ΔFvpex13.

Fig. 8. Proposed schematic model of F. v*erticillioides* peroxisome docking/translocation module (DTM).

The proposed model is based on our protein-protein interaction experiments as well as other published fungal models. Our study showed that these proteins are involved in the regulation of peroxisomal docking complex assembly and matrix translocation and ultimately impact various aspects of fungal development, secondary metabolism, and virulence. Notably, we determined that FvPex8 plays an important role in *F. verticillioides* mycotoxin biosynthesis. While we noticed distinct role each component plays, FvPex13 was the key components in regulating virulence, likely in close association with FvPex14 and FvPex33.

1 **SUPPLEMENTARY TABLES**

2

3 **Table S1.** Putative *F. verticillioides* DTM components identified by Blastp analysis

4

5 **Table S2.** *F. verticillioides* strains used in this study

6

7 **Table S3.** PCR primers used in this study

8

9 **SUPPLEMENTARY FIGURES**

10

11 **Figure S1. Sequence analysis of Docking peroxin homologs in *F. verticillioides***

12 (A) Schematic description of conserveds domain in peroxins FvPex13, FvPex14 and FvPex33. (B)
13 Phylogenetic relationship of FvPex33 and its homologs calculated with neighbor joining method
14 using the MEGA 6.0 program according to the alignment. (C) Possible transmembrane helices
15 predicted in FvPex8, FvPex13, FvPex14, and FvPex33 analyzed by TMPRED algorithm.

16

17 **Figure S2. Docking protein interaction by yeast two hybrid assays.**

18 Interactions between DTM peroxins were tested using the yeast two-hybrid assay. Yeast
19 transformants expressing plasmids harboring the indicated constructs were assayed for growth on
20 selective plates (SD/Leu/Trp/His/Ade), and for β-galactosidase (LacZ) activities. The pGBKT7-
21 53/pGADT7-T and pGBKT7-Lam/pGADT7-T was used as positive and negative control,
22 respectively.

23

Figure S3. Vegetative growth and growth inhibition of mutants on CMII agar.

(A) The colony morphology of DTM mutants and the wild-type strain on CMII agar and CMII amended with linoleic acid. (B) Mycelial growth inhibition rates were calculated by [(the diameter of WT strain - the diameter of mutant strain)/(the diameter of WT strain)]x100%. (C) conidiation in the wild type and DTM mutants on CMII agar. An asterisk above the column indicates a statistically significant difference ($P<0.05$) as anlyzed by t-test.

Figure S4. Reduction in lipid droplet degradation and carbon sources utilization

(A) Wild-type (WT) and mutant strains were grown for 2 days in rich medium, then transferred to 1% potassium acetate medium and stained with Nile red to observe the lipid droplet formation of the hyphae after starvation at 0 h and 18 h time points. (B) Lipid droplet gross area was measured in each sample at 0 h and 18 h time points. (C) Lipid droplet sizes were measured measured in each sample at 0 h and 18 h time points. Bars denote standard deviations from three repeated experiments. An asterisk above the column indicates a statistically significant difference ($P<0.05$) as anlyzed by t-test.

Figure S5. Role of DTM peroxins in sugarcane stalk rot virulence.

(A) Sugarcane stalks (cultivar Badila) were inoculated with fungal spore suspension (10^6/ml) at the internodal region and incubated in room temperature for 7 days. Subsequently, stalks were split longitudinally to visually inspect rot symptoms. (B) Image J software was used to quantify the extent of the rot in each sample. Three independent biological repetitions were performed and error bars represent the standard deviation from three replicates. An asterisk above the column indicates

a statistically significant difference ($P<0.05$) as anlyzed by t-test. (C) Sterile water was used as a negative control on maize stalk.

SUPPLEMENTARY INFORMATION

Supplementary Results and Supplementary Methods are provided in a separate document

Yu et al. Fig. 1

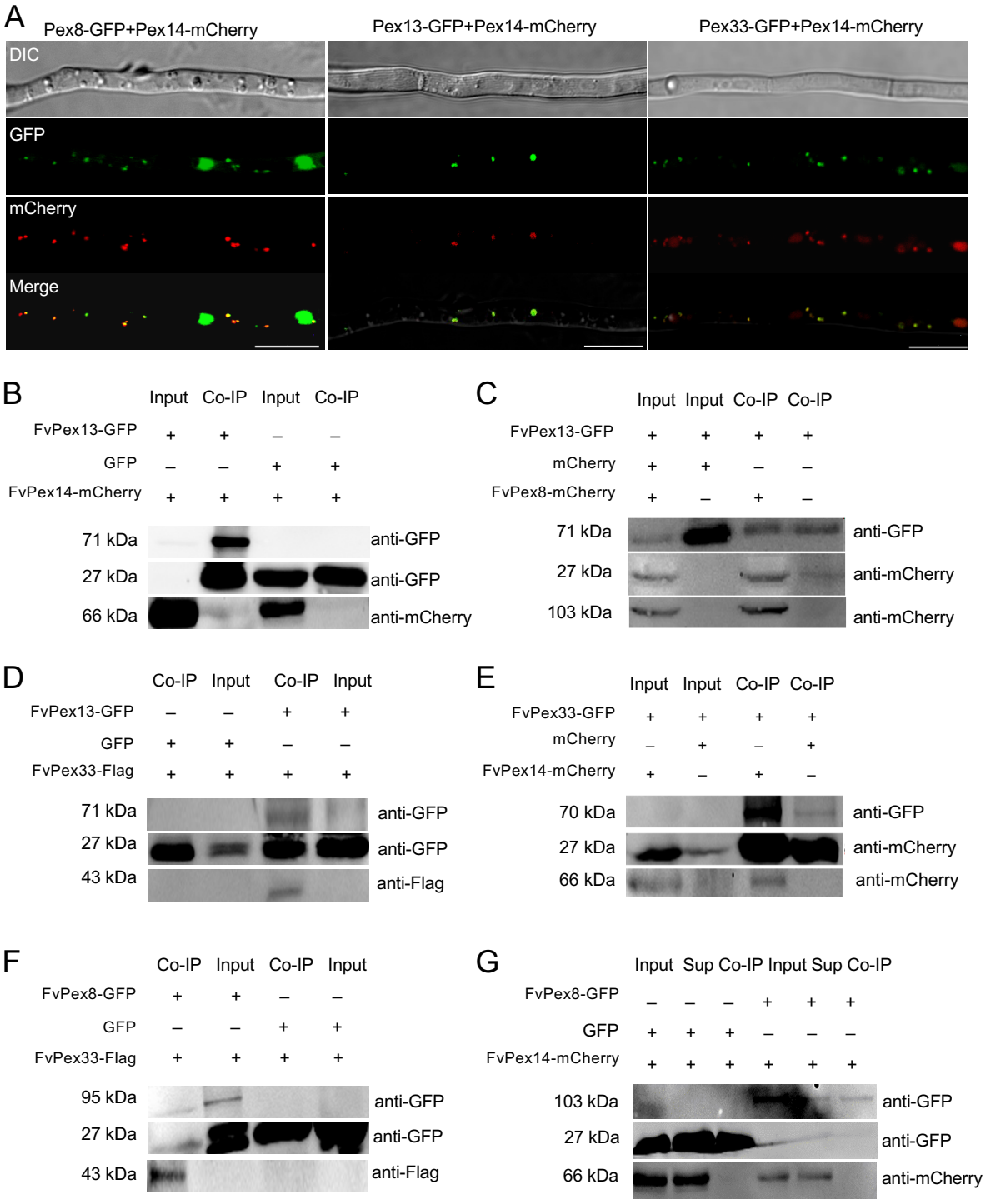
A
Pex8-GFP+Pex14-mCherry
Pex13-GFP+Pex14-mCherry
Pex33-GFP+Pex14-mCherry
DIC
GFP
mCherry
Merge
B
Input Co-IP Input Co-IP
FvPex13-GFP + + – –
GFP – – + +
FvPex14-mCherry + + + +
71 kDa anti-GFP
27 kDa anti-GFP
66 kDa anti-mCherry
C
Input Input Co-IP Co-IP
FvPex13-GFP + + + +
mCherry + + – –
FvPex8-mCherry + – + –
71 kDa anti-GFP
27 kDa anti-mCherry
103 kDa anti-mCherry
D
Co-IP Input Co-IP Input
FvPex13-GFP – – + +
GFP + + – –
FvPex33-Flag + + + +
71 kDa anti-GFP
27 kDa anti-GFP
43 kDa anti-Flag
E
Input Input Co-IP Co-IP
FvPex33-GFP + + + +
mCherry – + – +
FvPex14-mCherry + – + –
70 kDa anti-GFP
27 kDa anti-mCherry
66 kDa anti-mCherry
F
Co-IP Input Co-IP Input
FvPex8-GFP + + – –
GFP – – + +
FvPex33-Flag + + + +
95 kDa anti-GFP
27 kDa anti-GFP
43 kDa anti-Flag
G
Input Sup Co-IP Input Sup Co-IP
FvPex8-GFP – – – + + +
GFP + + + – – –
FvPex14-mCherry + + + + + +
103 kDa anti-GFP
27 kDa anti-GFP
66 kDa anti-mCherry

Yu et al. Fig. 2

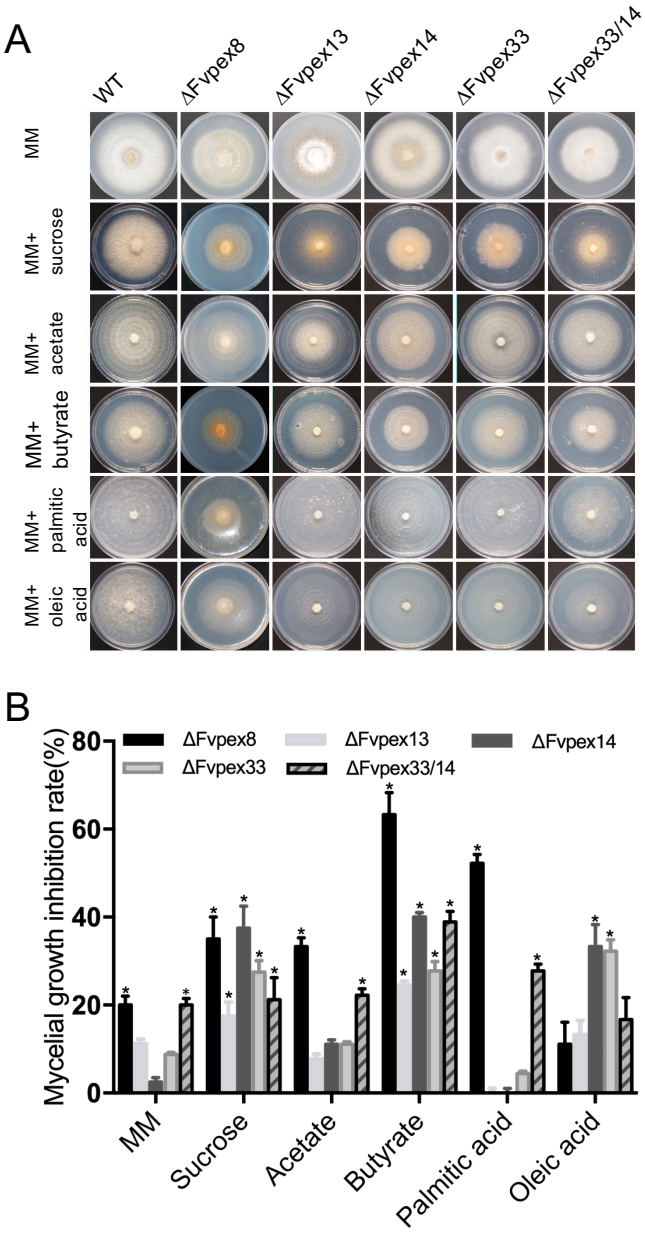
A
WT
ΔFvpex8
ΔFvpex13
ΔFvpex14
ΔFvpex33
ΔFvpex33/14
MM
MM+ sucrose
MM+ acetate
MM+ butyrate
MM+ palmitic acid
MM+ oleic acid
B
Mycelial growth inhibition rate(%)
ΔFvpex8
ΔFvpex13
ΔFvpex14
ΔFvpex33
ΔFvpex33/14
0
20
40
60
80
MM
Sucrose
Acetate
Butyrate
Palmitic acid
Oleic acid

Yu et al. Fig. 3

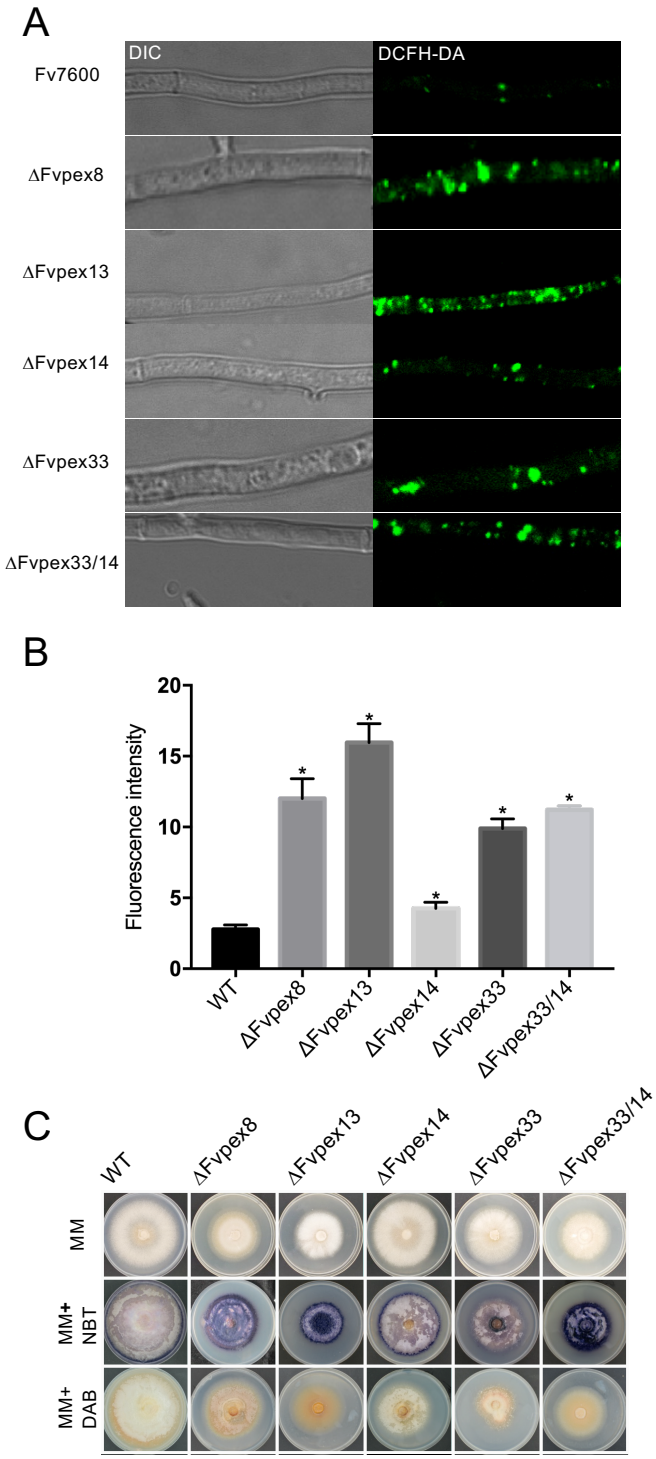
A
DIC
DCFH-DA
Fv7600
ΔFvpex8
ΔFvpex13
ΔFvpex14
ΔFvpex33
ΔFvpex33/14
B
Fluorescence intensity
20
15
10
5
0
WT
ΔFvpex8
ΔFvpex13
ΔFvpex14
ΔFvpex33
ΔFvpex33/14
C
WT
ΔFvpex8
ΔFvpex13
ΔFvpex14
ΔFvpex33
ΔFvpex33/14
MM
MM+ NBT
MM+ DAB

Yu et al. Fig. 4

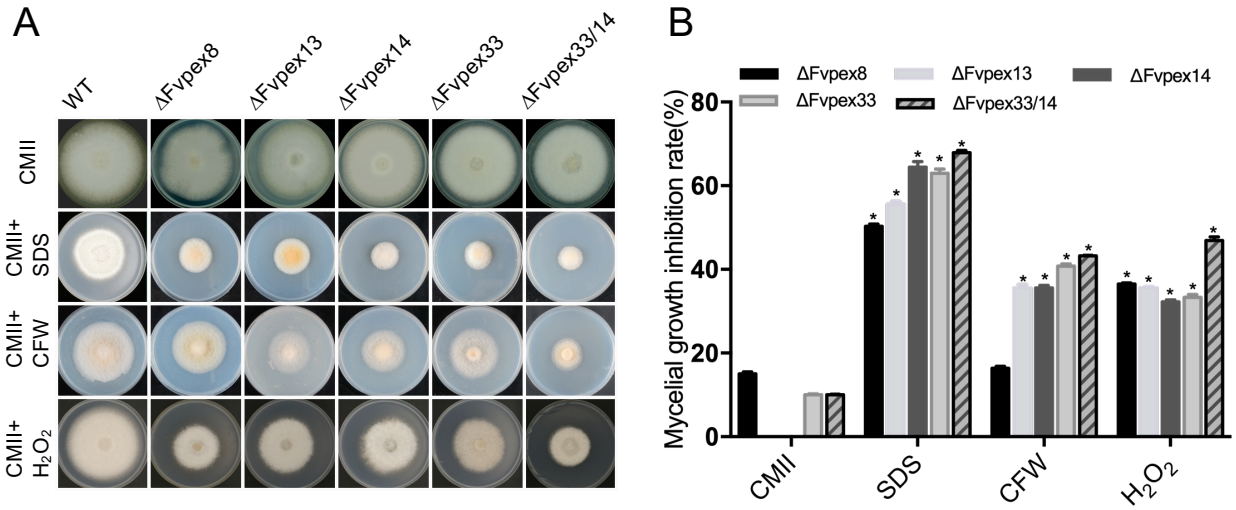
A
WT
ΔFvpex8
ΔFvpex13
ΔFvpex14
ΔFvpex33
ΔFvpex33/14
CMII
CMII+ SDS
CMII+ CFW
CMII+ H_2O_2
B
ΔFvpex8
ΔFvpex13
ΔFvpex14
ΔFvpex33
ΔFvpex33/14
Mycelial growth inhibition rate(%)
80
60
40
20
0
CMII
SDS
CFW
H_2O_2

Yu et al. Fig. 5

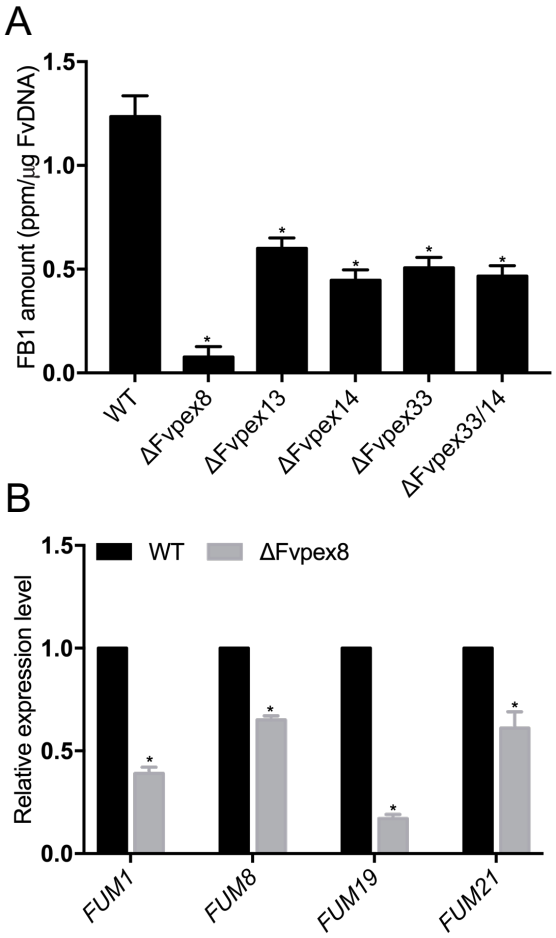
A
FB1 amount (ppm/μg FvDNA)
1.5
1.0
0.5
0.0
WT
ΔFvpex8
ΔFvpex13
ΔFvpex14
ΔFvpex33
ΔFvpex33/14
B
WT
ΔFvpex8
Relative expression level
1.5
1.0
0.5
0.0
FUM1
FUM8
FUM19
FUM21

Yu et al. Fig. 6

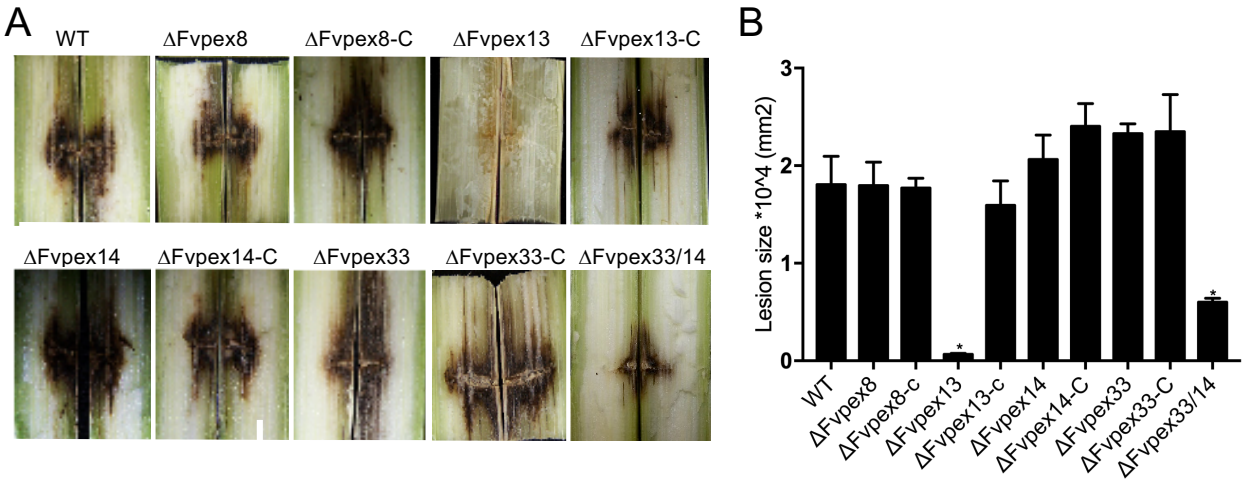
A
WT
ΔFvpex8
ΔFvpex8-C
ΔFvpex13
ΔFvpex13-C
ΔFvpex14
ΔFvpex14-C
ΔFvpex33
ΔFvpex33-C
ΔFvpex33/14
B
Lesion size *10^4 (mm2)
0
1
2
3
*
*
WT
ΔFvpex8
ΔFvpex8-c
ΔFvpex13
ΔFvpex13-c
ΔFvpex14
ΔFvpex14-C
ΔFvpex33
ΔFvpex33-C
ΔFvpex33/14

Yu et al. Fig. 7

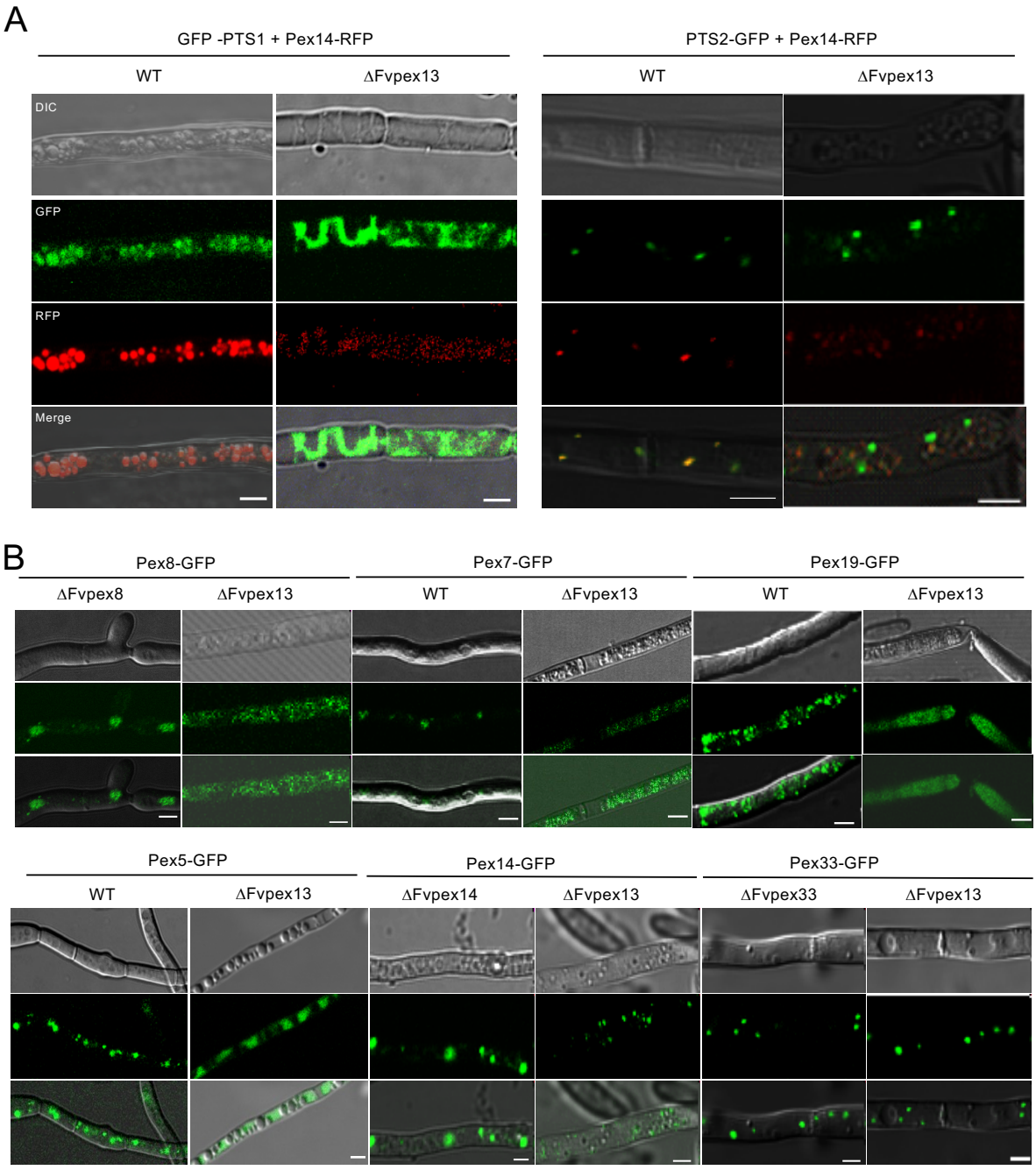
A
GFP -PTS1 + Pex14-RFP
WT
ΔFvpex13
PTS2-GFP + Pex14-RFP
WT
ΔFvpex13
DIC
GFP
RFP
Merge
B
Pex8-GFP
ΔFvpex8
ΔFvpex13
Pex7-GFP
WT
ΔFvpex13
Pex19-GFP
WT
ΔFvpex13
Pex5-GFP
WT
ΔFvpex13
Pex14-GFP
ΔFvpex14
ΔFvpex13
Pex33-GFP
ΔFvpex33
ΔFvpex13

Yu et al. Fig. 8

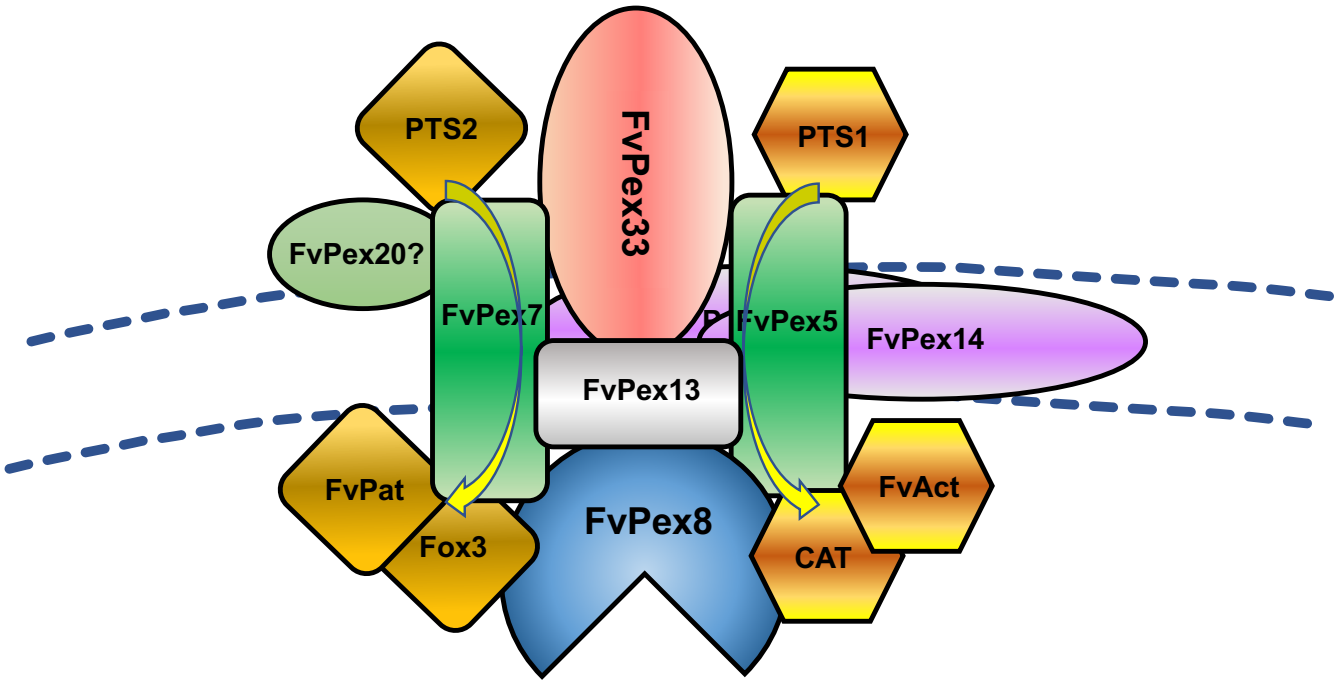
PTS2
FvPex33
PTS1
FvPex20?
FvPex7
FvPex5
FvPex14
FvPex13
FvPat
FvPex8
FvAct
Fox3
CAT